Advances in Computational Modeling of EMC/EMI Effects in Communication-Based Train Control (CBTC) Systems

Xingqi Zhang, *Member, IEEE*, Weibin Hou, and Costas D. Sarris, *Senior Member, IEEE*

***Abstract*—Communication-based train control (CBTC) systems are aimed at providing control and signaling for rail transportation. These operate in environments that include tunnel and open air sections, as well as busy stations, coexisting with Wi-Fi and cellular communication networks. Modeling electromagnetic compatibility and interference (EMC/EMI) issues in CBTC is most efficiently achieved by hybridizing several computational electromagnetic techniques rather than relying on a single one.**

This paper presents an overview of the applicable standards and some typical EMI scenarios for CBTC systems. Then, we discuss recent advances in hybridizing the vector parabolic equation (VPE) method, ray-tracing (RT) and the finite-difference time-domain (FDTD) technique, towards the efficient modeling of such scenarios.

***Index Terms*—Communication-based train control systems, electromagnetic compatibility and interference, radio wave propagation**

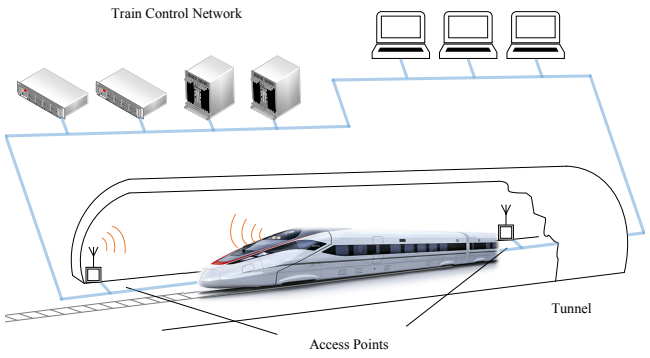

Fig. 1. Diagram of the CBTC system [6].

I. Introduction

As high-speed rail is expanding especially in large metropolitan areas, communications-based train control (CBTC) systems are being adopted as a contemporary means of rail signaling [1]–[7]. As illustrated in Fig. 1, a CBTC system is based on the real-time exchange of information (e.g., train location, speed, and direction) between the train and a central control station via a network of wayside access points (AP) deployed along the track. As a modern successor to conventional railway signaling systems that use track circuits, axle counters, and light signals, a CBTC system employs high-capacity and bi-directional radio communications to improve the capacity of railway network infrastructure and enhance the level of safety and service offered to customers.

In contrast to radio communications for non-safety-critical railway applications such as CCTV and on-board Internet, radio communications for CBTC systems impose stringent reliability and availability requirements [1]. Electromagnetic compatibility and interference (EMC/EMI) analysis plays a major role in ensuring reliable system operation, and it is a prerequisite for the deployment of CBTC systems. The railway environment contains many electromagnetic disturbance sources. Problems of electromagnetic interference arise not only within the locomotive and the traction power supplies, but also in associated signaling and communication systems. CBTC systems have been implemented as cost-effective IEEE 802.11 wireless local area networks (WLAN), mainly due to its cost-effectiveness [1], [2]. Various co-existing networks operating at or close to the same frequency (e.g., CBTC, Wi-Fi, and cellular) present themselves both as possible communication paths and as sources of interference to each other. This usually causes co-channel interference, which is detrimental to system performance and has the potential to cause railway accidents. Such interference is usually classified as a high risk to railway safety [8]. For example, CBTC system failures at Shenzhen Metro have been attributed to interference caused by Wi-Fi users in the surrounding areas [1].

Both CBTC signal strength and interference can be determined via a measurement campaign. However, this process is very resource-intensive. Also, the rapid and widespread proliferation of smart phones and other hand-held devices makes it non-trivial to accurately predict future interference levels. Evidently, high-fidelity simulation tools can effectively complement and accelerate a measurement campaign, leading to comprehensive models of CBTC signal propagation and associated EMC/EMI effects.

Two popular methods that have been extensively applied to radio wave propagation problems are ray-tracing (RT) and the vector parabolic equation (VPE) technique [9]–[16]. Moreover, full-wave techniques, such as the finite-difference time-domain (FDTD) method, have been employed to a lesser degree [17], [18]. Generally, each method has its inherent limitations and is more suitable for certain types of problems. For example, FDTD is versatile and applicable to arbitrarily complex geometries, such as the interior of a train including seats and passengers. In [19], [20], it was applied to analyze interference from adjacent floors on WLAN signals in a building. In [21]–[24], it was employed to compute the shielding effectiveness

of metallic enclosures. The drawback of the FDTD method is that it is generally very time-consuming for electrically large environments such as tunnels and subway stations. The RT method is relatively more efficient in solving electromagnetic wave propagation in geometries that consist of electrically large reflecting surfaces. In [25], it was applied to characterize radio wave propagation in a subway station, and in [26], it was applied to study how WLAN equipment placed inside a train affects CBTC access points nearby. However, in enclosed environments like tunnels, the presence of multiple reflections off the walls compromises the efficiency of RT. For long tunnel segments of arbitrary cross-section, the VPE technique can offer a robust alternative. VPE is based on the assumption that waves propagate close to the axis of the tunnel. On the other hand, it cannot be applied in rich scattering environments such as subway stations, where its basic assumptions are obviously invalid.

Therefore, different methods can be hybridized, with each method compensating for each other's drawbacks. The different sections of a generic guideway geometry and the corresponding technique that is most suitable for each one of them is shown in Fig. 2. The main idea is to apply FDTD (or another full-wave method), RT, and VPE to the modeling of wave propagation in regions around the train, subway stations, and closed/open tunnel sections, respectively.

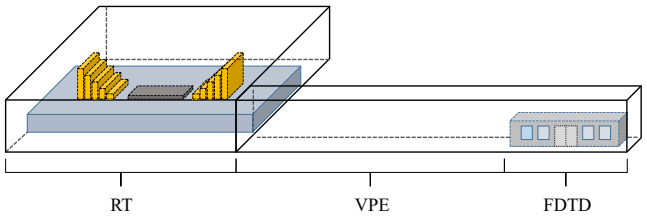

Fig. 2. Sections of a generic guideway geometry and the corresponding technique that is most suitable for each section.

The rest of the paper is organized as follows. Section II includes a brief review of EMC standards applicable to CBTC systems, along with the CBTC interpretation of standard metrics, such as the Signal to Interference Ratio (SIR) and Shielding Effectiveness (SE). Section III describes the three techniques that we hybridize, namely VPE, RT and FDTD. Section IV includes application examples of these techniques in realistic guideway case studies, along with measured data. Section V presents the main principles guiding the hybridization of these techniques. Finally, Section VI presents the application of hybrid modeling to the EMI-aware placement of Wi-Fi antennas in a subway station.

II. EMC/EMI Analysis in CBTC Systems

A. EMC/EMI Standards

The International Electrotechnical Commission (IEC), and its counterpart in Europe, European Committee for Electrotechnical Standardization (CENELEC), are generally responsible for the development of standards for the railway industry [1]. In addition, there is an IEEE CBTC standard providing guidelines on the operation of CBTC systems. The IEEE 1474.1 standard [27], originally published in 1999, defines performance and functional requirements for CBTC systems. Also, the IEEE 1474.3 standard [28], published in 2008, defines recommended practices for CBTC system design and function allocations.

There are also various standards specifically dealing with EMC/EMI issues for railway applications. Two major standards series are: CENELEC Standard EN 50121 - Railway Applications Electromagnetic Compatibility [29] and IEC 62236 [30] with the same title. The EN 50121 is a family of EMC standards, which regulates railway systems and applications on unintended emissions and immunities [8]. However, it does not explicitly limit the power radiated from the intentional transmitters of a CBTC system, or any other potentially interfering intentional transmitter. The emissions of CBTC systems in various environments shall comply with the relevant standards where applicable.

B. Evaluation Metrics

The following metrics can be used to evaluate electromagnetic interference in CBTC systems.

1) Signal to Interference Ratio (SIR): Generally, the access points of CBTC systems are deployed along the railway tunnel, and the transmitting/receiving equipment for co-existing networks (e.g., Wi-Fi, and cellular) is located at subway stations and open air sections. Since those networks typically work at the same frequency band, they can significantly interfere with each other. The interference from co-existing networks to CBTC systems can be quantified using a signal to interference ratio (SIR) [19], [20], which is defined as:

$$\mathrm{SIR} = \frac{|V_{\mathrm{CBTC}}|^2}{|V_{\mathrm{Interference}}|^2} \tag{1}$$

In (1), V_{CBTC} and $V_{\mathrm{Interference}}$ are the open-circuit voltages received at the train antenna contributed by the CBTC and interfering systems, respectively.

2) Shielding Effectiveness (SE): There are usually CCTV and on-board Internet networks inside the train carriage, providing wireless connectivity to passengers. CBTC systems can receive interference from such networks. The train carriage can be considered as a shielding enclosure that reduces interference from on-board networks to CBTC systems, and a shielding effectiveness (SE) [8], [31] can be defined as:

$$\mathrm{SE} = 20 \log \frac{|\mathbf{E}_0|}{|\mathbf{E}_1|} \tag{2}$$

where $|\mathbf{E}_0|$ and $|\mathbf{E}_1|$ are the electric field strengths obtained at the same point in the absence and presence of a shield (which is the train in this case).

III. Modeling Methodology

In recent years, advanced propagation models based on the FDTD, VPE, and RT methods [32]–[38] are being developed to characterize radio wave propagation in railway environments. In this section, an overview of these methods is provided along with numerical examples.

A. FDTD

FDTD is a full-wave method based on the solution of Maxwell's equations on a discrete grid [39], [40]. It inherently takes into account all effects such as radiation, reflection, and diffraction in complex geometries [17], [41]–[44]. Moreover, since the medium constitutive relations are automatically incorporated into the solution of Maxwell's equations, these methods are well-suited to study wave interactions in complex media.

In [45], the FDTD method was applied to model radio wave propagation in a region containing a train carriage. As illustrated in Fig. 3, a CBTC antenna, shown with a red circle, was placed by the window of a train carriage. The side and top view of the interior of the train carriage are shown in Fig. 3 (a) and Fig. 3 (b), respectively. There were 8 seats placed by the bilateral glass windows inside the train, and each seat was modeled as a plastic cushion mounted on a metal stand.

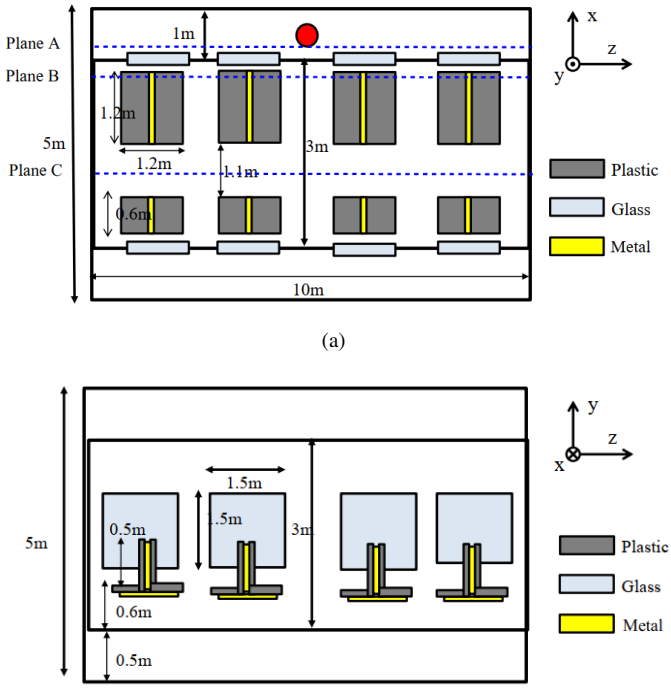

Fig. 3. The interior of a train carriage [45]. (a) Top view. (b) Side view.

The electric field distribution was evaluated using FDTD. In [45], the vertical electric field component, $|E_y|$, was computed on several planes, for an empty and a detailed interior train model. In Fig. 4, the first and second columns correspond to the empty and the detailed interior case, respectively. The first row corresponds to the electric field distribution obtained on plane A (as shown in Fig. 3) that was placed outside the train, at a distance of 0.16 m away from the window. The second and third rows correspond to the electric field distribution obtained on planes B and C that were placed inside the train, at a distance of 0.16 m and 2 m away from the window, respectively. The area of these planes was the same as that of the side of the carriage included in the computational domain. It can be observed that radio waves mainly leak into

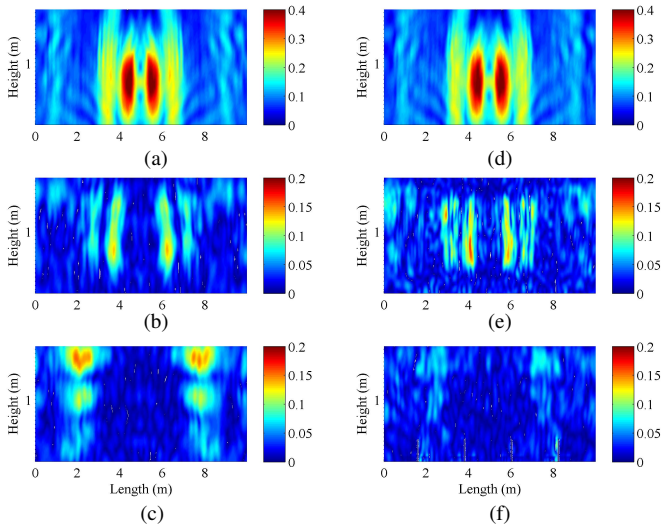

Fig. 4. The spatial distribution of the vertical electric field component [45]. The first and second columns correspond to the empty and the detailed interior case, respectively. (a) and (d) correspond to the electric field distribution obtained on plane A in Fig. 3. (b) and (e) correspond to the electric field distribution obtained on plane B. (c) and (f) correspond to the electric field distribution obtained on plane C.

the train through the windows that are close to the transmitting antenna. The field profile computed with the detailed interior model is very close to that of the empty interior model for the first sampling plane (Fig. 4a, d). However, visible differences can be observed between the two models for the other two sampling planes. Hence, the use of the detailed interior model is necessary for the accurate determination of shielding effectiveness, which is influenced by the complex multipath and absorption effects associated with the presence of the seats.

The shielding effectiveness of the train can be further evaluated using (2). In [45], the shielding effectiveness of the train in the case with and without a detailed interior was compared in Fig. 5. Note that the shielding effectiveness is a

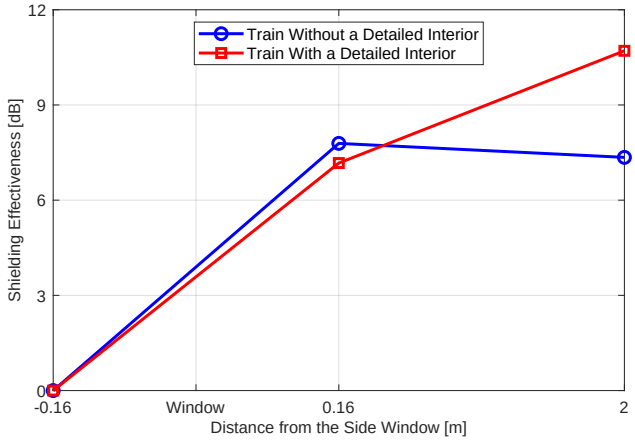

Fig. 5. The shielding effectiveness of the train in the case with and without a detailed interior [45].

position-dependent quantity, and the values obtained in Fig. 5 are averages over the sampling planes. It can be observed from Fig. 5 that the shielding effectiveness is similar in both cases, at a distance of 0.16 m from the side window inside the train. However, at a far distance (2 m away from the side window), the shielding effectiveness in the case with a detailed interior train model is about 3 dB larger than the other one. This is expected by inspection of the last two rows of Fig. 4, which indicate that the detailed interior model leads to smaller field amplitudes on the two sampling planes away from the window.

B. VPE

The VPE method, derived from the full-wave Helmholtz equation, has proved to be a computationally efficient and accurate approach to study radio wave propagation characteristics in long guiding structures such as tunnels [46], [47]. It has advantages similar to those of full-wave FDTD without requiring as much execution time or memory. It is based on the paraxial approximation [48], which assumes that electromagnetic waves propagate mainly along or close to the axis of the tunnel. This enables the reduction of the Helmholtz equation, from an elliptical equation into a parabolic equation with respect to the transverse components of the fields. The parabolic equation is solvable via implicit, unconditionally stable finite difference methods, such as the Alternating Direction Implicit (ADI) and the Crank-Nicolson (CN) method. These allow for the use of large discretization steps along the tunnel.

Over the last decade, many advanced techniques have been introduced to increase the flexibility of VPE-based models [49]–[54]. Full three-dimensional simulations of tunnels with arbitrary cross-sections have been reported [55], [56]. Moreover, coupled with tensor impedance boundary conditions [57], VPE can capture wave depolarization effects that play an important role in path loss calculations, especially in curved tunnels [52]. More recently, robust techniques have also been introduced to enable propagation modeling in tunnels with rough surface walls [58], [59].

In [35], VPE was applied to a tunnel section of the Light Rail Transportation (LRT) system in Edmonton, Alberta, Canada. The modeling environment is illustrated in Fig. 6. The transmitter, a vertically polarized Yagi antenna operating at 2.44 GHz, was placed at a height of 3.1 m and 0.2 m away from the side wall. There were two receivers, located at the center of the tunnel at a height of 3.1 m and 0.9 m apart. The comparison between the simulated and measured received power is shown in Fig. 7, where a good agreement is observed between measured and simulated data.

C. RT

The RT method, based on geometrical optics, can provide reasonably accurate predictions of wave propagation in arbitrary channel geometries [60]–[62]. In an RT-based model, electromagnetic fields are approximated as rays. Typically, multiple rays emanate from a transmitter and undergo a number of reflections and refractions before reaching a receiver. The total field at any given location is then computed as

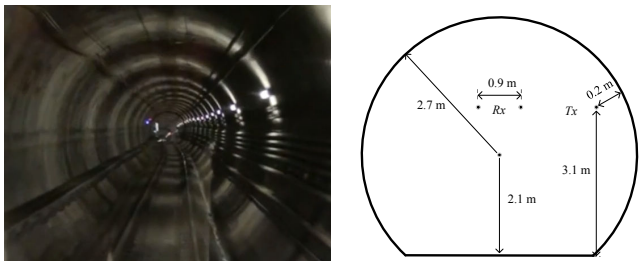

(a) (b)

Fig. 6. Edmonton railway tunnel [35]. (a) On-site image. (b) Cross-section geometry.

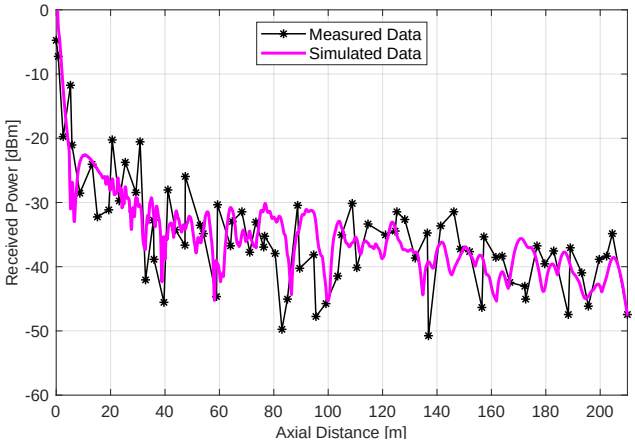

Fig. 7. Received power at 2.44 GHz in the Edmonton railway tunnel [35].

the superposition of fields from all ray paths, each having its own amplitude and phase. This coherent summation leads to constructive or destructive interference of the arriving ray paths at the receiver. The field calculation is valid only when the signal interacts with facets that are much larger than the wavelength. Even though RT-based models are not as accurate as full-wave models, they offer useful insights to study wave propagation in arbitrary geometries and provide a good trade-off between accuracy, computational cost, and generality.

In [25], RT was applied to a subway station selected from the LRT system in Edmonton, Alberta, Canada. As illustrated in Fig. 8, the modeling environment was very complicated, as it included an elevated platform, escalators, benches, ceilings, pillars, and railway tracks. The simulated received power agreed well with the measurement data, as shown in Fig. 9.

IV. Model Calibration

In simulation tools, the accuracy of the results depends on the quality of the input parameters. Selecting the input parameters is not always straightforward since most railway environments are complex as they involve an abundance of random scatterers which complicate the analysis. In this section, we discuss how input model parameters can be chosen practically and provide a specific route towards quantifying the impact of this choice on the accuracy of the computed results.

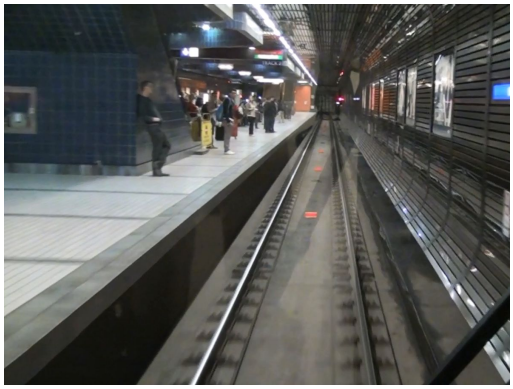

Fig. 8. On-site image of the Edmonton subway station [63].

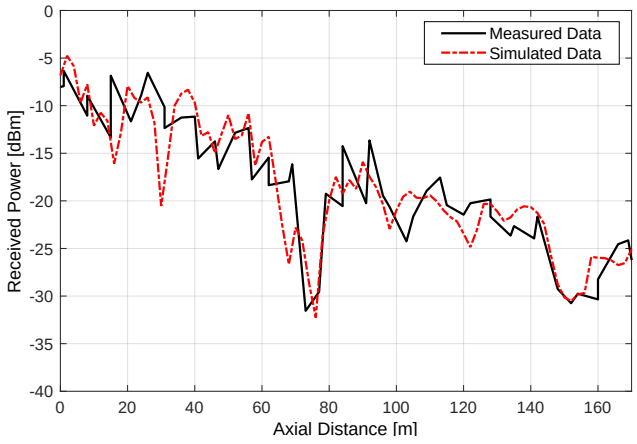

Fig. 9. Received power at 2.44 GHz in the Edmonton subway station [25].

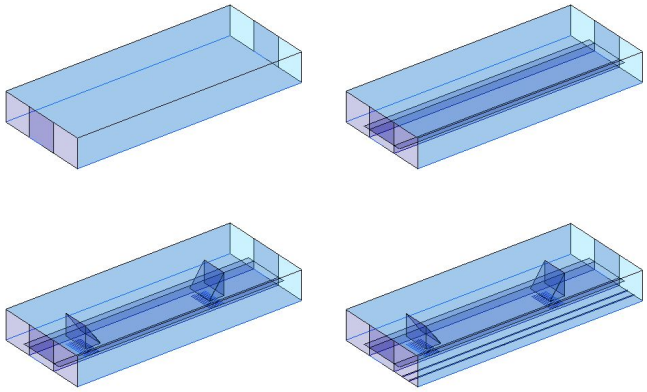

Fig. 10. Input geometry diagrams with incremental details for the Edmonton subway station [63].

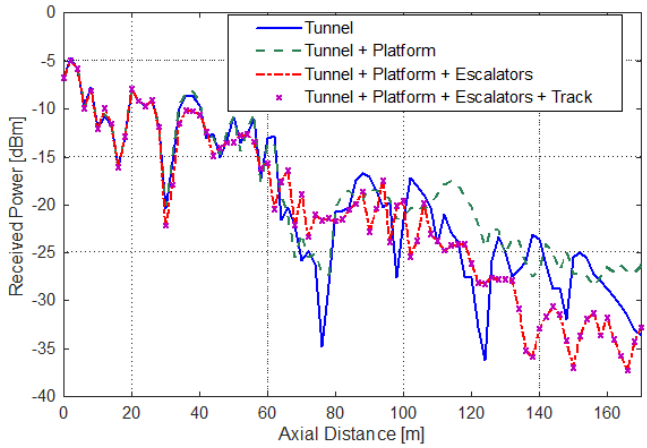

Fig. 11. Received power comparison by incrementally adding geometric details for the case study of the Edmonton subway station [63].

A. Input Model Extraction

In [63], an RT-based model was calibrated based on measurement data from the Edmonton subway station shown in Fig. 8. There were many geometric details complicating the specification of the input model. On one hand, the computational cost might increase significantly with the number of objects included in the model; on the other hand, a sufficient level of detail is required to guarantee the accuracy of simulation results. Therefore, the input geometry is usually extracted by systematically adding incremental details, as illustrated in Fig. 10, until there are minor or insignificant deviations in the numerical predictions.

The resulting deviations in the received power by incrementally adding the platform, the escalators, and the tracks, were compared in [63], as shown in Fig. 11. For this subway station, the platform and escalators were found to be the primary scattering objects that affected the propagation characteristics. More objects could be added, yet the deviations proved insignificant while unnecessarily increasing the computational cost.

Besides including the main objects, the wall properties needed to be estimated. As can be seen from the on-site image shown in Fig. 8, the walls present in this scenario mainly consisted of large blocks of concrete. However, certain areas, such as the bilateral walls of the station, as well as part of the ceilings, were metallic instead of concrete. With these wall materials properly extracted, the agreement between the measurement data and the RT prediction was improved significantly, as illustrated in Fig. 12.

B. Sensitivity Analysis

Generally, exact values such as dimensions and material properties are difficult to obtain and considerable uncertainty can exist in the description of the modeling environment, introducing uncertainty in the predictions.

In [64], a polynomial chaos expansion (PCE) method was applied to examine uncertainty in VPE-based models. The considered environment was the Edmonton tunnel discussed in Section III.B. The considered uncertain input parameters were summarized as in Table I. The mean values and 90 % confidence intervals of the received power computed using PCE were compared against measurement data, as shown in Fig. 13.

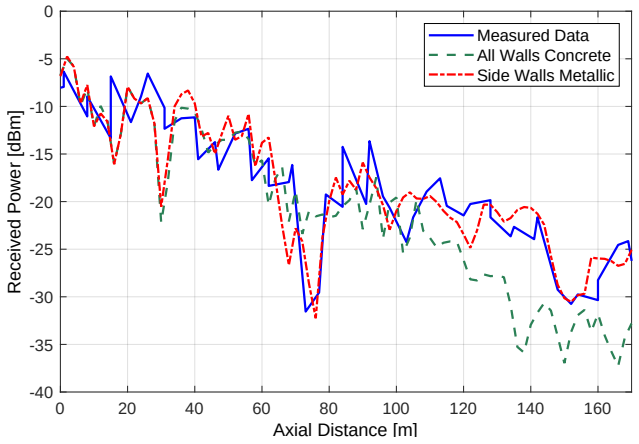

Fig. 12. Received power comparison with different wall properties for the case study of the Edmonton subway station [63].

TABLE I
UNCERTAIN INPUT PARAMETERS IN THE PROPAGATION MODEL.

Random Input	Nominal Value	Distribution
Transmitter Height, h_{Tx}	3.1 m	Gaussian, $\sigma = 0.05$
Transmitter Lateral Position, l_{Tx}	2.3 m	Gaussian, $\sigma = 0.05$
Receiver Height, h_{Rx}	3.1 m	Gaussian, $\sigma = 0.05$
Separation of Receivers, l_{Rx}	0.9 m	Gaussian, $\sigma = 0.05$
Relative Permittivity, ε_r	9	Gaussian, $\sigma = 0.5$
Conductivity, σ_0	0.1 S/m	Gaussian, $\sigma = 0.03$

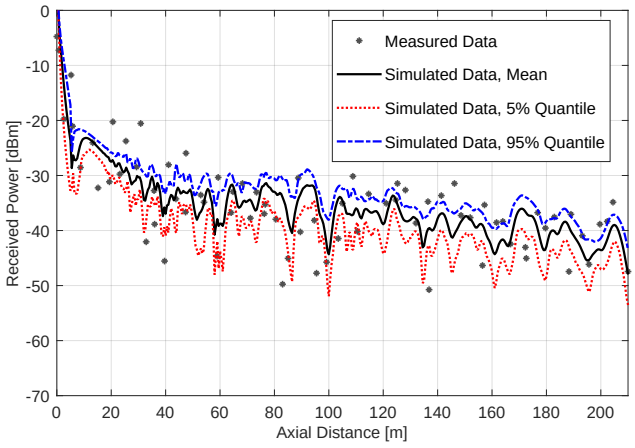

Fig. 13. The mean values and 90 % confidence intervals of the received power [64].

The results showed that the variations in the received power could be considerable for relatively small input parameter uncertainties, leading to the conclusion that a single simulation run using nominal values might be insufficient to adequately characterize the wireless channel in tunnel environments. The relative contribution of each input parameter to the total uncertainty in the received power was compared in [64], as shown in Fig. 14. Uncertainties in the height and lateral position of the transmitter introduced more uncertainty in the received power, as expected, since the transmitter was placed close to the side wall. The results also indicated that uncertainties in the electrical properties of tunnel walls had relatively little effect.

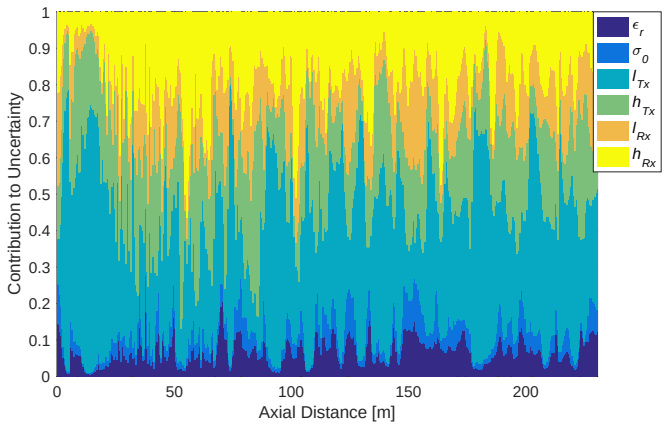

Fig. 14. Relative contribution of each input parameter to the total uncertainty in the received power as a function of distance [64].

V. HYBRIDIZATION OF MODELING METHODS

A diagram of the EMC/EMI scenarios that can be modeled more effectively using hybrid methods is shown in Fig. 15. In particular, a hybrid RT/FDTD method can be applied to evaluate the interference from WLAN at subway stations to on-board CBTC systems; a hybrid FDTD/VPE method can be applied to evaluate the interference from on-board WLAN devices to CBTC access points in tunnels; a hybrid RT/VPE method can be applied to evaluate the interference from WLAN at subway stations to CBTC access points in tunnels. Note that those hybrid methods, through reversing the hybridization sequence, can be applied to evaluate interference from CBTC systems to co-existing networks as well.

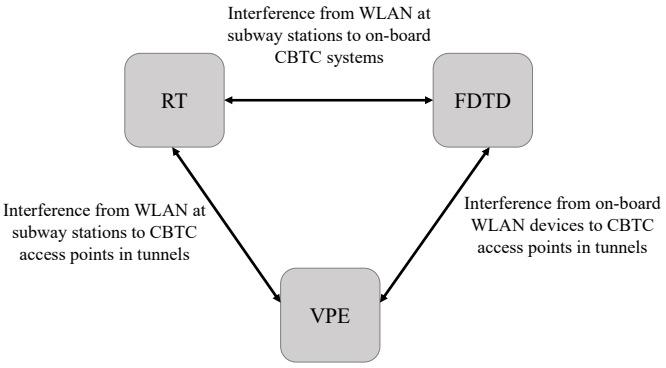

Fig. 15. Diagram of the EMC/EMI scenarios that can be modeled more effectively using hybrid methods.

A. Hybridization of RT and FDTD Methods

When a train is close to a subway station, the interference from Wi-Fi networks at subway stations to the CBTC antennas on the train can be evaluated through a hybrid RT/FDTD method. As shown in Fig. 16, the environment can be divided

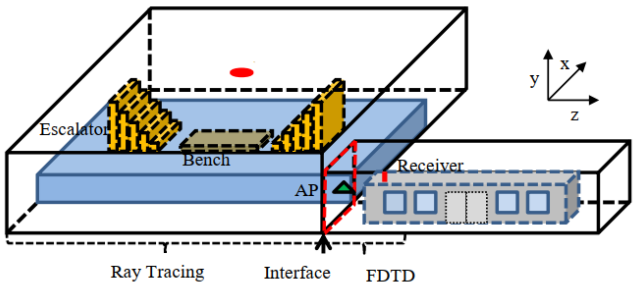

Fig. 16. Computational domain for the problem of interference from Wi-Fi networks at subway stations to the CBTC antennas on the train [45]. The red dashed rectangle represents the interface between the RT and FDTD simulation sub-domains. The red circle represents a Wi-Fi antenna. The green triangle represents a CBTC access point.

in two sub-domains, which include the subway station and the tunnel, respectively. The red dashed rectangle in Fig. 16 represents the interface between the two sub-domains. The RT method can be applied for the modeling of the subway station region, and the FDTD method can be used to evaluate fields around the train in the tunnel region.

The interface is generally placed at the beginning of the tunnel section [45]. At the interface, the fields generated by RT are used as initial conditions for FDTD [65], [66]. The spatial discretization steps chosen in RT are larger than those used in FDTD. Therefore, the electric fields extracted from RT can be interpolated with a bilinear interpolation from a coarser RT grid to a denser FDTD grid. Details and validation for the hybrid RT/FDTD method can be found in [45], [66].

B. Hybridization of FDTD and VPE Methods

The interference from on-board Wi-Fi networks to CBTC access points in tunnels can be evaluated through a hybrid FDTD/VPE method. As shown in Fig. 17, the tunnel can be divided in two sub-domains: one containing a short section that includes part of a train and the other containing a long uniform tunnel section.

Fields in the first and second sub-domains can be evaluated via the FDTD and VPE methods, respectively. The VPE method is applied to the second sub-domain, since it is not applicable once the interaction with the train is considered. At the interface of the two sub-domains, the fields generated by FDTD are used as initial conditions for VPE. Details and validation for the hybridization of VPE and FDTD can be found in [45], [66].

C. Hybridization of RT and VPE Methods

The interference from Wi-Fi networks at subway stations to CBTC access points in tunnels can be evaluated through a

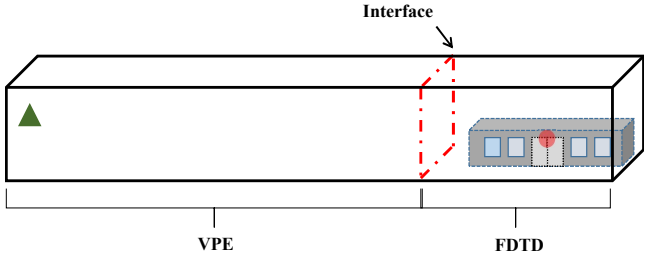

Fig. 17. Computational domain for the problem of interference from on-board Wi-Fi networks to a CBTC access point. The red dashed rectangle represents the interface between the FDTD and VPE simulation sub-domains. The red circle represents an on-board Wi-Fi antenna. The green triangle represents a CBTC access point.

hybrid RT/VPE method. The principle is to strategically subdivide a propagation channel geometry in two main subdomains – one containing complex geometrical features simulated using RT and the other consisting primarily of long, uniform tunnel sections evaluated using VPE, as shown in Fig. 18.

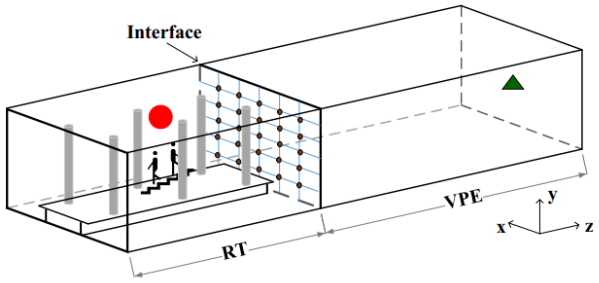

Fig. 18. Computational domain for the problem of interference from Wi-Fi networks at subway stations to CBTC access points in tunnels [63]. The red circle represents a Wi-Fi antenna. The green triangle represents a CBTC access point.

At the interface of the two subdomains, the electric fields computed through RT are used as the initial conditions needed for VPE. The interface is placed within a uniform section. To determine where to place the interface for the first case, both the accuracy and the efficiency of the hybrid model need to be taken into account. Details and validation for the hybrid RT/VPE method can be found in [63].

VI. Application: Interference of Co-Existing Networks to CBTC Systems and Interference Mitigation

As discussed in [45], the level of interference of Wi-Fi networks to CBTC systems at or near a subway station can be studied using the hybrid models introduced in the previous section. Based on this analysis, the positions of Wi-Fi antennas can be optimized to mitigate this interference. Fig. 19 shows a diagram of the scenario studied in [45], where a subway

station was connected with a tunnel section. The Wi-Fi antenna (shown with a red circle) was placed on the ceiling of a station, and a CBTC access point (shown with a green triangle) was at the entrance of the tunnel following the station. This environment resembled the Edmonton railway environment.

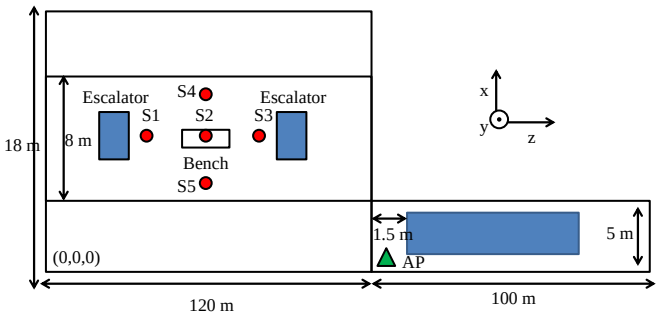

Fig. 19. Top view of the computational domain for the problem of interference of Wi-Fi networks to CBTC systems at or near a subway station [45].

The subway station was 120 m long and the single-track tunnel section was 100 m long. The cross-section dimensions of the subway station were 18 m × 7 m. The electrical parameters of the walls were chosen as $\epsilon_r = 5$, $\sigma_0 = 0.01$ S/m. The platform in the subway station had a width of 8 m. There were two escalators and a bench on the platform, which were at a distance of 26 m, 86 m and 55 m from the beginning of the station, respectively. The dimensions and electrical parameters for the platform, escalator and bench are summarized in Table II, where L, W and H are the length, width and height, respectively.

TABLE II
DESCRIPTION OF THE OBJECTS ON THE PLATFORM IN THE SUBWAY STATION ENVIRONMENT.

Object	$L\,[m] \times W\,[m] \times H\,[m]$	ϵ_r	σ_0 [S/m]
Escalator	5×5×5.8	1	3×10^8
Bench	10×2×0.8	5	0.01
Platform	120×8×1.2	5	0.01

The cross-section dimensions of the single-track tunnel were 5 m×5 m. There was a train located at a distance of 1.5 m away from the platform, as shown in Fig. 19. The receiving antenna and the front of the train are shown in Fig. 20. There were two receiving antennas (denoted as Rx 1 and Rx 2 in Fig. 20) mounted on the top of the train, which were 0.9 m apart.

The transmitting antenna for the Wi-Fi system was a 30 dBm vertically polarized dipole antenna at 2.4 GHz. The antenna was placed at various locations to investigate its impact on the performance of the CBTC system. Five different locations (S1-S5), shown with red dots in Fig. 19, were considered for the placement of the Wi-Fi antennas. The height of the antenna was fixed 0.5 m away from the ceiling of the station. The access point of the CBTC system was a 20 dBm vertically polarized dipole antenna working at the same frequency. The

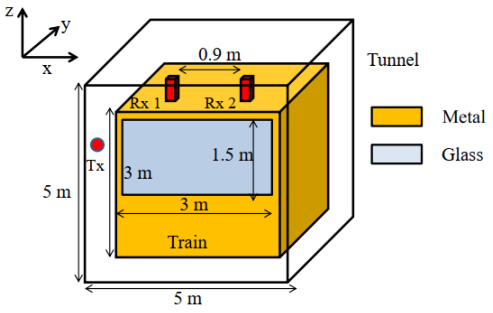

Fig. 20. The front of train model used in the FDTD simulation [45].

antenna, shown with a green triangle in Fig. 19, was placed 0.5 m away from the side wall of the tunnel, at a height of 3.1 m.

The hybrid RT/FDTD method, discussed in Section V, was applied. The electric field strength of the Wi-Fi system when the Wi-Fi antenna was placed at points S1 to S5 was evaluated. Subsequently, the SIR from Wi-Fi systems to the CBTC system was calculated according to (1). The SIR when the Wi-Fi antenna was placed at different locations was compared in [45], as shown in Fig. 21. It can be observed that when the Wi-Fi antenna was placed at S3, the associated SIR was maximum, and hence the interference from Wi-Fi to CBTC systems was minimum.

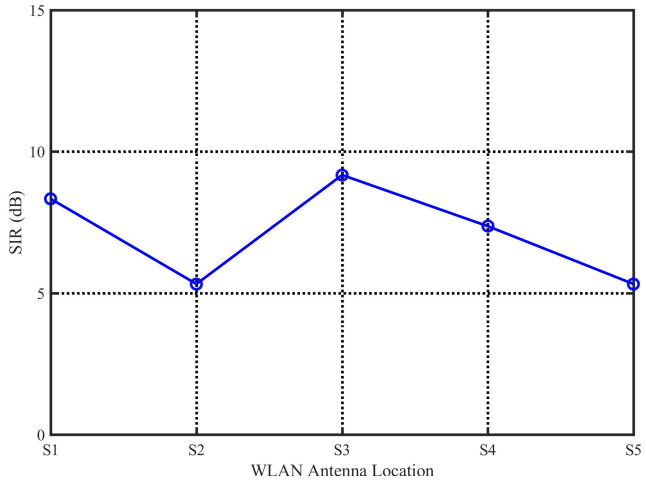

Fig. 21. The SIR when the Wi-Fi antenna is placed at different locations [45].

VII. CONCLUSION

This paper presented recent advances towards the computational modeling of signal propagation and associated EMC/EMI effects in CBTC systems. The EMC/EMI effects stem from the coexistence of CBTC systems with Wi-Fi and cellular communication networks, operating in geometrically diverse environments including tunnel and open air sections, and busy stations. These are most efficiently modeled by hybridizing several computational electromagnetic techniques rather than relying on a single one. We showed examples of

such hybrid methods, where RT was applied to complex station geometries, the VPE technique was reserved for long tunnel sections, whereas full-wave methods (FDTD in this paper) were employed to model the exterior and interior geometry of trains.

As new generation systems are being explored and deployed along guideways, the interest in modeling the signal propagation and the associated EMC/EMI effects in CBTC systems will continue to include 5/6 G systems. To that end, the extension of hybrid methods (of the type we presented here) to millimeter-wave and THz frequencies is bound to attract significant attention.

REFERENCES

[1] J. Farooq and J. Soler, "Radio communication for communications-based train control (CBTC): A tutorial and survey," *IEEE Communications Surveys Tutorials*, vol. 19, no. 3, pp. 1377–1402, 2017.

[2] F. R. Yu, *Advances in Communications-Based Train Control Systems*. CRC Press, 2015.

[3] L. Zhu, F. R. Yu, B. Ning, and T. Tang, "Design and performance enhancements in communication-based train control systems with coordinated multipoint transmission and reception," *IEEE Trans. Intell. Transp. Syst.*, vol. 15, no. 3, pp. 1258–1272, June 2014.

[4] N. Sood, S. Baroudi, X. Zhang, J. Liebeherr, and C. D. Sarris, "Integrating physics-based wireless propagation models and network protocol design for train communication systems," *IET Microwaves, Antennas and Propagation*, vol. 13, pp. 1065–1071, July 2019.

[5] X. Zhang, N. Sood, S. Baroudi, J. Liebeherr, and C. D. Sarris, "Full integration of physics-based propagation models into network protocol design for communication-based train control systems," *IEEE MTT-S Int. Wireless Symp. (IWS)*, pp. 1–3, May 2018.

[6] X. Zhang, A. Ludwig, N. Sood, and C. D. Sarris, "Physics-based optimization of access point placement for train communication systems," *IEEE Trans. Intell. Transp. Syst.*, vol. 19, no. 9, pp. 3028–3038, September 2018.

[7] N. Sood, S. Baroudi, X. Zhang, J. Liebeherr, and C. D. Sarris, "Integrating physics-based wireless propagation models and network protocol design for train communication systems," *IEEE Trans. Antennas Propag.*, vol. 66, no. 12, pp. 6635–6645, December 2018.

[8] A. M. Ade Ogunsola, *Electromagnetic Compatibility in Railways*. Springer-Verlag Berlin Heidelberg, 2013.

[9] N. Sood, A. Ludwig, X. Zhang, F. Bouwman, P. Nowicki, C. Bantin, J. Siu, and C. D. Sarris, "Modeling and optimization of coverage in London underground subway tunnels," *IEEE Int. Symp. on Antennas and Propag.*, pp. 87–88, July 2015.

[10] N. Sood, X. Zhang, S. Baroudi, J. Liebeherr, and C. D. Sarris, "A new way to integrate physics-based channel models in communication system design," *IEEE Int. Symp. on Antennas and Propag.*, pp. 553–554, July 2018.

[11] Y. Hwang, Y. P. Zhang, and R. G. Kouyoumjian, "Ray-optical prediction of radio-wave propagation characteristics in tunnel environments. part 1: Theory," *IEEE Trans. Antennas Propag.*, vol. 46, no. 9, pp. 1328–1336, September 1998.

[12] Y. P. Zhang, Y. Hwang, and R. G. Kouyoumjian, "Ray-optical prediction of radio-wave propagation characteristics in tunnel environments. Part 2: analysis and measurements," *IEEE Trans. Antennas Propag.*, vol. 46, no. 9, pp. 1337–1345, September 1998.

[13] N. Sood, S. Baroudi, X. Zhang, J. Liebeherr, and C. D. Sarris, "Configuration of network level algorithms for wireless train control systems using physics-based propagation models," in *IEEE International Symposium on Antennas and Propagation and USNC-URSI Radio Science Meeting*, 2019, pp. 1265–1266.

[14] X. Zhang, N. Sood, and C. D. Sarris, "Fast radio-wave propagation modeling in tunnels with a hybrid vector parabolic equation/waveguide mode theory method," *IEEE Trans. Antennas Propag.*, vol. 66, no. 12, pp. 6540–6551, December 2018.

[15] X. Zhang, N. Sood, J. Siu, and C. D. Sarris, "Efficient propagation modeling in railway environments using a hybrid vector parabolic equation/ray-tracing method," *IEEE Int. Symp. on Antennas and Propag.*, pp. 1680–1681, July 2015.

[16] X. Zhang, N. Sood, and C. D. Sarris, "Propagation modeling in complex tunnel environments: A comparison of vector parabolic equation and ray-tracing solutions," *Int. Conference on Electromagn. in Advanced Applications (ICEAA)*, pp. 1676–1679, September 2017.

[17] L. A. R. Ramirez, F. J. V. Hasselmann, and Y. P. Zhang, "Channel characteristics in tunnels: FDTD simulations and measurement," *J. Microwaves, Optoelectronics and Electromagn. Applications*, vol. 10, pp. 121–130, 2011.

[18] Y. Zhao, Y. Hao, and C. Parini, "FDTD characterization of UWB indoor radio channel including frequency dependent antenna directivities," *IEEE Antennas and Wireless Propag. Lett.*, vol. 6, pp. 191–194, 2007.

[19] A. C. M. Austin, M. J. Neve, and G. B. Rowe, "Modelling interference for indoor wireless systems using the FDTD method," *2009 IEEE Antennas and Propagation Society International Symposium*, pp. 1–4, June 2009.

[20] A. C. M. Austin and C. D. Sarris, "Ultra-wideband interference modelling for indoor wireless channels using the FDTD method," *Proceedings of the 2012 IEEE International Symposium on Antennas and Propagation*, pp. 1–2, July 2012.

[21] Y. Duan, B. Chen, L. Zhang, and H. Chen, "Shielding effectiveness of metal door in circular tunnel to non-unclear EMP," *2007 International Symposium on Electromagnetic Compatibility*, pp. 190–193, Oct 2007.

[22] M. Li, K.-P. Ma, D. M. Hockanson, J. L. Drewniak, T. H. Hubing, and T. P. V. Doren, "Numerical and experimental corroboration of an FDTD thin-slot model for slots near corners of shielding enclosures," *IEEE Transactions on Electromagnetic Compatibility*, vol. 39, no. 3, pp. 225–232, Aug 1997.

[23] L. Zhu, Q. Wang, J. Yu, and Q. Gu, "A hybrid method based on FDTD for simulation of far field from opening in shielding enclosure," *IEEE Transactions on Magnetics*, vol. 42, no. 4, pp. 859–862, April 2006.

[24] C. Jiao, L. Li, X. Cui, and H. Li, "Subcell FDTD analysis of shielding effectiveness of a thin-walled enclosure with an aperture," *IEEE Transactions on Magnetics*, vol. 42, no. 4, pp. 1075–1078, April 2006.

[25] X. Zhang, N. Sood, J. Siu, and C. D. Sarris, "Calibration of a 3-D ray-tracing model in railway environments," *IEEE Int. Symp. on Antennas and Propag.*, pp. 89–90, July 2015.

[26] X. Li, Q. Song, H. Tao, X. Liu, S. Zhang, X. Wang, Q. Luo, and X. Peng, "Evaluation on anti-interference to WLAN equipments for spatial deployment of CBTC systems in tunnels," *2014 IEEE/CIC International Conference on Communications in China (ICCC)*, pp. 47–52, Oct 2014.

[27] *IEEE Standard for Communications-Based Train Control (CBTC) Performance and Functional Requirements*. IEEE Std 1474.1, 1999.

[28] *IEEE recommended practice for Communications-Based Train Control (CBTC) system design and functional allocations*. IEEE Std 1474.3, 2008.

[29] *EN 50121: Railway applications - Electromagnetic compatibility*. European Committee for Electrotechnical Standardization, Brussels, Belgium, 2006.

[30] *IEC 62236: Railway applications - Electromagnetic compatibility*. European Committee for Electrotechnical Standardization, Brussels, Belgium, 2008.

[31] H. Ott, *Electromagnetic Compatibility Engineering*. Wiley Publishing, 2009.

[32] A. Hrovat, G. Kandus, and T. Javornik, "A survey of radio propagation modeling for tunnels," *IEEE Communications Surveys & Tutorials*, vol. 16, no. 2, pp. 658–669, 2014.

[33] X. Zhang and C. D. Sarris, "Enabling accurate modeling of wave propagation in complex tunnel environments with the vector parabolic equation method," *IEEE Int. Symp. on Antennas and Propag.*, pp. 549–550, July 2018.

[34] Y. Liu, A. Ghazal, C.-X. Wang, X. Ge, Y. Yang, and Y. Zhang, "Channel measurements and models for high-speed train wireless communication systems in tunnel scenarios: a survey," *Science China Information Sciences*, vol. 60, no. 10, pp. 1–17, March 2017.

[35] X. Zhang and C. D. Sarris, "Vector parabolic equation-based derivation of rectangular waveguide surrogate models of arched tunnels," *IEEE Trans. Antennas Propag.*, vol. 66, no. 3, pp. 1392–1403, March 2018.

[36] A. Seretis, X. Zhang, and C. D. Sarris, "Uncertainty quantification of radio propagation models using artificial neural networks," in *IEEE International Symposium on Antennas and Propagation and USNC-URSI Radio Science Meeting*, 2019, pp. 229–230.

[37] A. Seretis, X. Zhang, K. Zeng, and C. D. Sarris, "Artificial neural network models for radiowave propagation in tunnels," *IET Microwaves, Antennas and Propagation*, vol. 14, no. 11, pp. 1198–1208, September 2020.

[38] X. Zhang and C. D. Sarris, "Vector parabolic equation modeling of wireless propagation in tunnels with statistically rough surface walls," *Int. Applied Computational Electromagn. Society Symp. (ACES)*, pp. 1–2, March 2018.
[39] A. Taflove and S. C. Hagness, *Computational Electrodynamics: The Finite-difference Time-domain Method*, ser. Artech House antennas and propagation library. Artech House, 2005.
[40] S. D. Gedney, *Introduction to the Finite-Difference Time-Domain (FDTD) Method for Electromagnetics*. Morgan & Claypool Publishers, 2011.
[41] M. Thiel and K. Sarabandi, "3D-wave propagation analysis of indoor wireless channels utilizing hybrid methods," *IEEE Trans. Antennas Propag.*, vol. 57, no. 5, pp. 1539–1546, May 2009.
[42] Y. Wang, S. Safavi-Naeini, and S. K. Chaudhuri, "A hybrid technique based on combining ray tracing and FDTD methods for site-specific modeling of indoor radio wave propagation," *IEEE Trans. Antennas Propag.*, vol. 48, no. 5, pp. 743–754, May 2000.
[43] X. Wei, X. Zhang, N. Diamanti, and C. D. Sarris, "A spatially-filtered FDTD sub-gridding scheme for ground penetrating radar scenarios," *IEEE Int. Symp. on Antennas and Propag.*, pp. 2391–2392, July 2017.
[44] X. Wei, X. Zhang, N. Diamanti, W. Shao, and C. D. Sarris, "Subgridded FDTD modeling of ground penetrating radar scenarios beyond the courant stability limit," *IEEE Trans. Geosci. Remote Sens.*, vol. 55, no. 12, pp. 7189–7198, December 2017.
[45] W. Hou, X. Zhang, J. Wang, and C. D. Sarris, "Hybrid numerical modeling of electromagnetic interference in train communication systems," *IEEE Transactions on Electromagnetic Compatibility*, vol. 62, no. 3, pp. 715–724, 2020.
[46] A. V. Popov, V. A. Vinogradov, N. Y. Zhu, and F. M. Landstorfer, "3D parabolic equation model of EM wave propagation in tunnels," *Electron. Lett.*, vol. 35, no. 11, pp. 880–882, May 1999.
[47] R. Martelly and R. Janaswamy, "An ADI-PE approach for modeling radio transmission loss in tunnels," *IEEE Trans. Antennas Propag.*, vol. 57, no. 6, pp. 1759–1770, June 2009.
[48] M. Levy, *Parabolic Equation Methods for Electromagnetic Wave Propagation*. London, U.K.: Inst. Elect. Eng., 2000.
[49] X. Zhang and C. D. Sarris, "A high-accuracy ADI scheme for the vector parabolic equation applied to the modeling of wave propagation in tunnels," *IEEE Antennas and Wireless Propag. Lett.*, vol. 13, pp. 650–653, April 2014.
[50] R. Martelly and R. Janaswamy, "Modeling radio transmission loss in curved, branched and rough-walled tunnels with the ADI-PE method," *IEEE Trans. Antennas Propag.*, vol. 58, no. 6, pp. 2037–2045, June 2010.
[51] X. Zhang and C. D. Sarris, "A Gaussian beam approach for embedding antennas into vector parabolic equation based propagation models," *IEEE Int. Symp. on Antennas and Propag.*, pp. 2105–2106, June 2016.
[52] P. Bernardi, D. Caratelli, R. Cicchetti, V. Schena, and O. Testa, "A numerical scheme for the solution of the vector parabolic equation governing the radio wave propagation in straight and curved rectangular tunnels," *IEEE Trans. Antennas Propag.*, vol. 57, no. 10, pp. 3249–3257, October 2009.
[53] X. Zhang and C. D. Sarris, "A Gaussian beam approximation approach for embedding antennas into vector parabolic equation based wireless channel propagation models," *IEEE Trans. Antennas Propag.*, vol. 65, no. 3, pp. 1301–1310, March 2017.
[54] X. Zhang and C. D. Sarris, "Extending waveguide mode theory based propagation models to arched rough wall tunnels," *IEEE Int. Symp. on Antennas and Propag.*, pp. 1331–1332, July 2018.
[55] A. V. Popov and N. Y. Zhu, "Modeling radio wave propagation in tunnels with a vectorial parabolic equation," *IEEE Trans. Antennas Propag.*, vol. 48, no. 9, pp. 1403–1412, September 2000.
[56] X. Zhang and C. D. Sarris, "Error analysis and comparative study of numerical methods for the parabolic equation applied to tunnel propagation modeling," *IEEE Trans. Antennas Propag.*, vol. 63, no. 7, pp. 3025–3034, July 2015.
[57] R. Cicchetti and A. Faraone, "Exact surface impedance/admittance boundary conditions for complex geometries: theory and applications," *IEEE Trans. Antennas Propag.*, vol. 48, no. 2, pp. 223–230, February 2000.
[58] X. Zhang and C. D. Sarris, "Statistical modeling of electromagnetic wave propagation in tunnels with rough walls using the vector parabolic equation method," *IEEE Trans. Antennas Propag.*, vol. 67, no. 4, pp. 2645–2654, April 2019.
[59] X. Zhang and C. D. Sarris, "Rigorous statistical modeling of propagation in tunnels with rough surface walls," *IEEE Int. Symp. on Antennas and Propag.*, pp. 1751–1752, July 2018.
[60] N. Sood, L. Liang, S. V. Hum, and C. D. Sarris, "Ray-tracing based modeling of ultra-wideband pulse propagation in railway tunnels," *IEEE Int. Symp. on Antennas and Propag.*, pp. 2383–2386, July 2011.
[61] G. E. Athanasiadou and A. R. Nix, "A novel 3-D indoor ray-tracing propagation model: the path generator and evaluation of narrow-band and wide-band predictions," *IEEE Trans. Veh. Technol.*, vol. 49, no. 4, pp. 1152–1168, July 2000.
[62] T. E. Athanaileas, G. E. Athanasiadou, G. V. Tsoulos, and D. I. Kaklamani, "Parallel radio-wave propagation modeling with image-based ray tracing techniques," *Parallel Computing*, vol. 36, no. 12, pp. 679 – 695, 2010.
[63] X. Zhang, N. Sood, J. K. Siu, and C. D. Sarris, "A hybrid ray-tracing/vector parabolic equation method for propagation modeling in train communication channels," *IEEE Trans. Antennas Propag.*, vol. 64, no. 5, pp. 1840–1849, May 2016.
[64] X. Zhang and C. D. Sarris, "Uncertainty quantification of vector parabolic equation based wireless channel models using polynomial chaos expansion," *IEEE Int. Symp. on Antennas and Propag.*, pp. 547–548, July 2018.
[65] Y. Wang, S. Safavi-Naeini, and S. K. Chaudhuri, "A hybrid technique based on combining ray tracing and FDTD methods for site-specific modeling of indoor radio wave propagation," *IEEE Transactions on Antennas and Propagation*, vol. 48, no. 5, pp. 743–754, May 2000.
[66] W. Hou, J. Wang, and Y. Li, "A hybrid method of FDTD and vector parabolic equation for radio wave propagation prediction in tunnels," *2017 IEEE International Symposium on Antennas and Propagation USNC/URSI National Radio Science Meeting*, pp. 1639–1640, July 2017.

Xingqi Zhang (S'14-M'18) received the B.Sc. degree in communication engineering from the Harbin Institute of Technology, Harbin, China, in 2012, and the M.A.Sc. and Ph.D. degrees in electrical and computer engineering from the University of Toronto, Toronto, Canada, in 2014 and 2018, respectively.

He is currently an Assistant Professor in the School of Electrical and Electronic Engineering, University College Dublin, Dublin, Ireland. He is also affiliated with the Department of Electrical and Computer Engineering, University of Toronto, Toronto, Canada, as a Visiting Professor. His research interests cover the fundamental and applied aspects of computational electromagnetics and wireless communications. A particular focus is on wireless channel modeling and optimization in indoor, urban, and terrestrial environments, multiphysics/multiscale modeling, stochastic uncertainty quantification and machine learning, EMC/EMI analysis, as well as antenna/RF design & measurement.

Weibin Hou was born in Hebei, China. He received the Ph.D. degree in electronic science and technology from Beijing Jiaotong University, Beijing, China, in 2019. From September 2017 to September 2018, he was a Visiting Student with the Department of Electrical and Computer Engineering, University of Toronto, Toronto, ON, Canada. He is currently working with the China Academy of Information and Communications Technology. His research interests include 5G wireless technology, electromagnetic compatibility, antennas and radio wave propagation. He received the Best Paper Award at MAPE 2015.

Costas D. Sarris (SM'08) received the M.Sc. degree in applied mathematics and the Ph.D. degree in electrical engineering from the University of Michigan, Ann Arbor, MI, USA, in 2002.

He is currently a Full Professor at the Department of Electrical and Computer Engineering, University of Toronto, Toronto, ON, Canada. His current research interests include numerical electromagnetics, with an emphasis on multiscale computational methods, modeling under stochastic uncertainty, and the applications of numerical methods to wireless channel modeling, wave propagation in complex media and metamaterials, wireless power transfer, and electromagnetic compatibility/interference problems.

Dr. Sarris was a recipient of the IEEE MTT-S 2013 Outstanding Young Engineer Award. He was the TPC Chair of the 2015 IEEE AP-S International Symposium on Antennas and Propagation and CNC/USNC Joint Meeting, the TPC Vice-Chair of the 2012 IEEE MTT-S International Microwave Symposium, and the Chair of the MTT-S Technical Committee on Field Theory (MTT-15). He is the Editor-in-Chief of the IEEE JOURNAL ON MULTISCALE AND MULTIPHYSICSCOMPUTATIONAL TECHNIQUES. He served as an Associate Editor for the IEEE TRANSACTIONS ON MICROWAVE THEORY AND TECHNIQUES from 2009 to 2013 and the IEEE MICROWAVE AND WIRELESS COMPONENTS LETTERS from 2007 to 2009.